ACS central science

Research Article

Cite This: ACS Cent. Sci. 2018, 4, 504−511

Direct Measurement of the Local Glass Transition in Self-Assembled Copolymers with Nanometer Resolution

Dane Christie,[†] Richard A. Register,*[,†,‡] and Rodney D. Priestley*[,†,‡]

[†]Department of Chemical and Biological Engineering, [‡]Princeton Institute for the Science and Technology of Materials, Princeton University, Princeton, New Jersey 08544, United States

Supporting Information

ABSTRACT: Nanoscale compositional heterogeneity in block copolymers can impart synergistic property combinations, such as stiffness and toughness. However, until now, there has been no experimental method to locally probe the dynamics at a specific location within these structured materials. Here, this was achieved by incorporating pyrene-bearing monomers at specific locations along the polymer chain, allowing the labeled monomers' local environment to be interrogated via fluorescence. In lamellar-forming poly(butyl methacrylate-*b*-methyl methacrylate) diblock copolymers, a strong gradient in glass transition temperature, T_g, of the higher-T_g block, 42 K over 4 nm, was mapped with nanometer resolution. These measurements also revealed a strongly asymmetric influence of the domain interface on T_g, with a much smaller dynamic gradient being observed for the lower-T_g block.

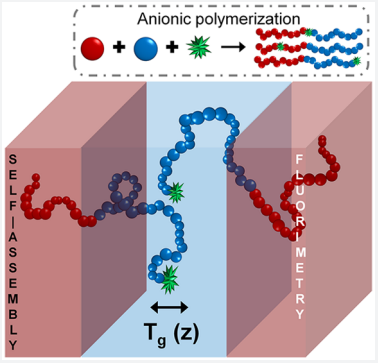

INTRODUCTION

Block copolymers, which self-assemble into nanodomain structures due to the incompatibility of chemically dissimilar monomer segments, have generated intense scientific interest and are used in a myriad of important technologies.[1] In such systems, a large fraction of the polymer segments can lie within a few nanometers of an internal interface, within a region where the dynamics and mechanical properties can be strongly modified from their bulk values.[2−5] The molecular dynamics at these soft internal interfaces can modulate the performance characteristics of copolymers and enable them to escape traditional material property trade-offs, such as those between stiffness and toughness,[6] that set limits on the performance of homogeneous polymers. Block copolymers, therefore, offer material solutions to address pressing societal challenges, including the upgrading of mixed plastic waste to a tough material,[7] thermoplastic elastomers with self-healing capability,[8] and nanostructured polymer solar cells[9,10] for more efficient harvesting of solar energy.

The ability to characterize the dynamics near the internal interfaces within block copolymers could enable the rational design of polymers with prescribed interfacial properties for next-generation applications. In addition, these same insights would advance our fundamental understanding of the complex ways in which interfaces and nanoscale confinement can influence the dynamics of polymers in technologically important macroscopic materials, i.e., block copolymers. At macroscopic or bulk length scales, the dynamic response is a composite of contributions from the dissimilar domains, their interdependence, and the presence of the internal interfaces. Decoupling these different contributions requires the ability to independently measure the dynamics of each block over length scales ranging from that of a few segments to that of the confining length scale or domain period where interfacial effects would be observed.

However, despite decades of both experimental and theoretical progress in understanding the thermodynamic nature of the interface within block copolymers, for example, the composition profile,[11,12] the field still lacks a predictive understanding of how dynamics are perturbed at the interface. An enduring barrier impeding a complete mapping of dynamics at and near interfaces within block copolymers is an inability to directly probe, at the nanoscale and with high resolution, interfacial phenomena. The challenge is especially acute because the length scale of block copolymer self-assembly is of O(10 nm). Overcoming this challenge holds promise for a conceptual leap in our understanding of how dynamics are altered at the interface, and beyond, in block copolymers.

Here, direct characterization of interfacial dynamics, as quantified by the glass transition temperature (T_g), across the domain period of lamella-forming diblock copolymers of poly(butyl methacrylate-*b*-methyl methacrylate), PBMA−PMMA, is presented. The direct and location-specific measurement of T_g in diblock copolymers is enabled by the precise placement of a fluorescent pyrene-containing monomer along the chain, at defined positions along either the PBMA or PMMA block, via anionic polymerization. This permits control of the spatial position of the fluorescent label when the copolymer self-assembles into a nanostructured material. Sparse labeling of the copolymer (<0.5 mol % at any position along the chain), combined with the high sensitivity of fluorescence

Received: January 16, 2018
Published: February 27, 2018

DOI: 10.1021/acscentsci.8b00043
ACS Cent. Sci. 2018, 4, 504−511

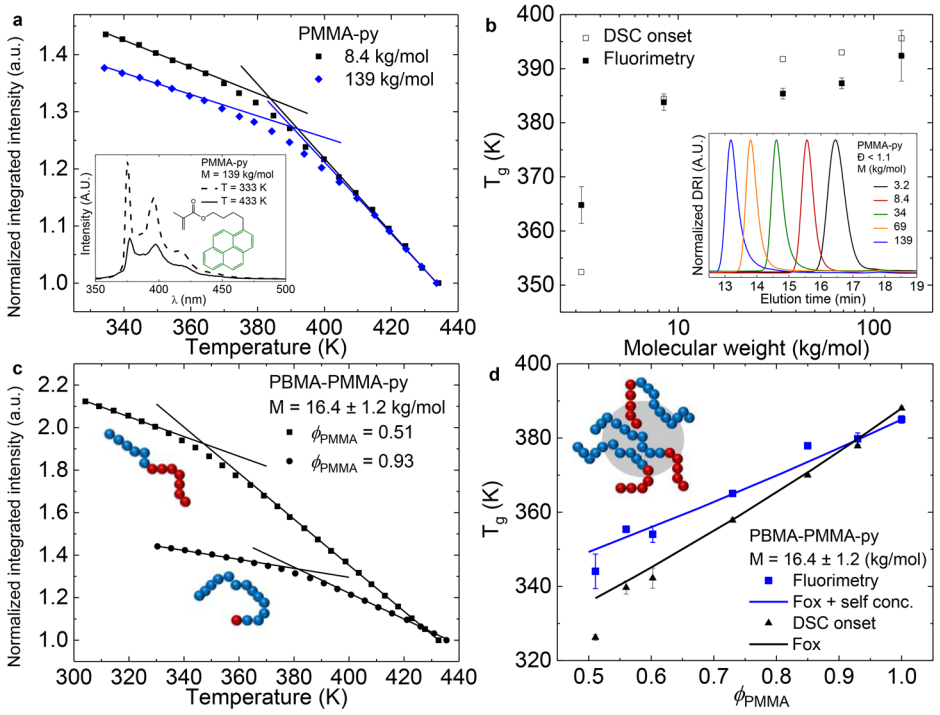

Figure 1. (a) Temperature dependence of the integrated fluorescence emission intensity of pyrene-labeled PMMA homopolymers (PMMA-py) of two different number-average molecular weights (M) and the corresponding linear fits in the glassy and rubbery regions. Inset, fluorescence emission spectra of PMMA-py (M = 139 kg/mol) at temperatures above and below T_g. The labeled monomer structure is also shown. (b) The molecular weight dependence of T_g for PMMA homopolymers, as determined by fluorescence or differential scanning calorimetry (DSC). Inset, gel permeation chromatography (GPC) traces of the series of PMMA-py homopolymers. (c) Temperature dependence of the fluorescence intensity of homogeneous PBMA−PMMA-py (M = 16 ± 1 kg/mol) diblocks with different compositions, where pyrene labels are attached randomly along the PMMA (blue) block. (d) T_g as a function of PMMA volume fraction in homogeneous PBMA−PMMA-py diblock copolymers. Inset, schematic of self-concentration of PMMA monomer units (blue) in a volume (gray) defined by the length of a Kuhn segment.

to sense the glass transition, enables a nanometer-accuracy spatial resolution of T_g at prescribed distances away from the domain interface.

A gradient in PMMA-block T_g of 42 K is found over a length scale of ∼4 nm, thus revealing the extreme case of dynamic heterogeneity in copolymers. The gradient can be understood by considering the local composition experienced by each block within the domain structure, crucially combined with nanoscale confinement effects on T_g. The role of the relative softness of the confining and confined blocks is demonstrated by a comparison of the observed T_g to values calculated based the Lodge−McLeish (LM) model of self-concentration.

RESULTS AND DISCUSSION

The ability of fluorescence to sense the T_g in the present polymers is corroborated by performing two sets of validation experiments. In the first set of experiments, T_g of PMMA homopolymers is measured as a function of the number-average molecular weight (M) via both fluorescence and differential scanning calorimetry (DSC). Both measurement techniques should reflect the strong M-dependence of T_g below a critical value.[13] To measure T_g by fluorescence, the temperature dependence of the fluorescence intensity of PMMA labeled with pyrene randomly along the chain (PMMA-py) was monitored (see Figure S3b). The inset of Figure 1a shows the fluorescence spectra for PMMA-py (M = 139 kg/mol), excited at 347 ± 0.5 nm at temperatures of 433 (solid line) and 333 K (dashed line), above and below the bulk T_g, respectively. A decrease in temperature yields an increase in fluorescence intensity due to reduced thermal energy and densification of the surrounding nanoscale medium.[14] Both effects reduce the rate of nonradiative decay of the excited-state pyrene fluorophore, a pathway competing with fluorescence during relaxation to the electronic ground state. We exploited the strong sensitivity of pyrene fluorescence intensity to the nanoscale medium to measure T_g. Figure 1a plots the integrated fluorescence intensity normalized to that at 433 K, as a function of temperature for two PMMA-py polymers with different values of M. The intersection of linear fits to the data at high and low temperatures provides an accurate measure of T_g.[15−17]

To confirm this assertion, the M-dependence of T_g for PMMA-py, as measured by fluorescence, was compared with the onset T_g as measured by DSC in Figure 1b. Over an M range of 8−139 kg/mol, the fluorescence-determined T_g is on average 4 K lower than the DSC onset T_g. At the lowest value of M, the trend is reversed, with a 12 K difference between the two techniques. Despite this difference, both techniques display the strong M-dependence of T_g expected for PMMA.[18] The sensitivity of fluorescence to the T_g of a pyrene-labeled PBMA homopolymer (PBMA-py) was also confirmed (see Figure S3a). The consistency of the trends combined with prior reports[19−21] confirmed the ability of the fluorescence method to sense T_g in bulk homopolymers.

In a second set of experiments, the dynamics of a single block in the diblock copolymer as perceived by fluorescence were characterized by selectively labeling that block. The T_g in a set of homogeneous diblock copolymers of PBMA−PMMA, wherein the PBMA and PMMA blocks are intimately mixed, with varying PMMA volume fraction (ϕ_{PMMA}), was measured

DOI: 10.1021/acscentsci.8b00043
ACS Cent. Sci. 2018, 4, 504−511

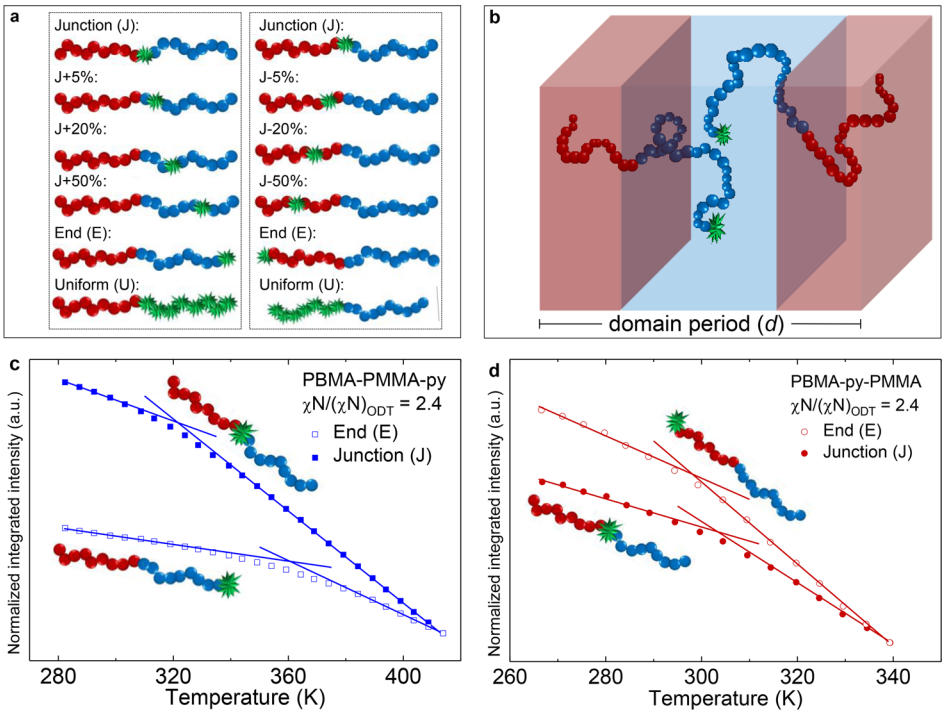

Figure 2. Fluorescence characterization of self-assembled PBMA−PMMA diblock copolymers. (a) Schematic of the selective labeling (green) of a lamella-forming PBMA−PMMA (red-blue) diblock copolymer. (b) Schematic of a self-assembled lamellar PBMA−PMMA diblock copolymer, where the label is placed at the end (E) of the PMMA block. (c) Temperature dependence of the integrated fluorescence emission intensity and the corresponding linear fits in the glassy and rubbery regions of junction- and end-labeled PBMA−PMMA ($\chi N/(\chi N)_{ODT}$ = 2.4), where the pyrene labels are attached to the PMMA block. (d) Analogous to (c) with pyrene labels attached to the PBMA block.

by both fluorescence and DSC. The segregation strength (χN) for all of the homogeneous diblock copolymers, relative to χN for a hypothetical symmetric copolymer (ϕ_{PMMA} = 0.5) at the order−disorder transition ($(\chi N)_{ODT}$), was estimated as $\chi N/(\chi N)_{ODT}$ = 0.7, where χ represents the Flory interaction parameter and N the total degree of polymerization (see the SI for the estimation of χN). The pyrene-labeled monomer was randomly (statistically uniformly) incorporated throughout the PMMA block of each diblock copolymer (PBMA−PMMA-py). Figure 1c plots the normalized integrated intensity vs temperature and the linear fits, which identify T_g for homogeneous PBMA−PMMA-py diblock copolymers with two different values of ϕ_{PMMA}. The composition dependence of T_g as determined by fluorescence (squares) or the DSC onset (triangles) is plotted for all samples investigated in Figure 1d. Both values systematically decrease as the content of PMMA within the copolymer is reduced. The $T_g(\phi)$ data obtained by DSC could be satisfactorily represented by the well-known Fox eq 1:[22]

$$\frac{1}{T_g(\phi_{PMMA})} = \frac{\phi_{PMMA}}{T_{g,PMMA}} + \frac{1-\phi_{PMMA}}{T_{g,PBMA}} \quad (1)$$

where $T_{g,PBMA}$ = 296 K and $T_{g,PMMA}$ = 388 K (at M = 22 kg/mol) are the DSC onset values measured on the homopolymers. In sharp contrast, $T_g(\phi)$ data obtained by fluorimetry could not be fit to eq 1 with the T_g values determined by fluorimetry for the homopolymers of the two blocks. Instead, as illustrated in Figure 1d, the data could be well-fit to the LM model of self-concentration.[23] Self-concentration is a consequence of the chain connectivity of monomer units in a homogeneous polymer mixture. It may be expressed as the local volume fraction (ϕ_s) occupied by segments of the same chain in a polymer blend, or the same block, in a homogeneous block copolymer. The dynamics of the mixture are defined within a nanoscale volume, where chemically identical segments exhibit an effective concentration (ϕ_{eff}) greater than the bulk, eq 2:

$$\phi_{eff} = \phi_s + (1-\phi_s)\phi \quad (2)$$

The effective T_g of a component in the mixture is then determined by evaluating eq 1 at ϕ_{eff}. The LM model provided an excellent fit with $\phi_{s,PMMA}$ = 0.38, where T_g for PBMA and PMMA were 289 and 385 K, as determined by fluorescence on the component homopolymers, see the SI for the estimation of ϕ_s. Therefore, fluorescence senses the effective T_g of a labeled block within a homogeneous block copolymer.

Figure 2a schematically shows the chain architecture for a series of 12 near-symmetric PBMA−PMMA diblock copolymers (M = 54 ± 9 kg/mol (±1 standard deviation of all 12, details in Table S1), dispersity ($Đ$) ≤ 1.1, and $\chi N/(\chi N)_{ODT}$ = 2.4), in which pyrene was attached at a specific location along either polymer block by employing sequential anionic polymerization. PBMA−PMMA diblock copolymers were prepared in which pyrene was located along the chain at positions varying from the block junction (J) to the chain end (E), or randomly within a particular block (uniformly labeled, U), as illustrated in Figure 2a. The spatial control of the label in the self-assembled copolymer is schematically shown in Figure 2b, where the label is placed at the end of the PMMA block. In all cases the local pyrene fraction within labeled sections of the copolymer was less than 0.5 mol %; the balance of the monomer units in the labeled section were either PMMA (left column in Figure 2a) or PBMA (right column in Figure 2a). These sets of selectively labeled copolymers allowed for the direct mapping of the

DOI: 10.1021/acscentsci.8b00043
ACS Cent. Sci. 2018, 4, 504−511

gradient in dynamics in the self-assembled, nanostructured polymer.

Figure 2c plots representative normalized integrated fluorescence intensity vs temperature data for the PBMA–PMMA copolymer, in which the pyrene label was attached either on the PMMA side of the block junction (filled squares) or at the end of the PMMA block (open squares). There is a strong location dependence of T_g along the PMMA block: for the polymer labeled at the chain end, $T_{g,E}$ = 364 K, while for the polymer labeled at the block junction, $T_{g,J}$ = 322 K, representing a 42 K range in local T_g along the PMMA block. Conversely, Figure 2d shows representative fluorescence data in which pyrene was attached on the PBMA side of the block junction (filled circles) or at the end of the PBMA block (open circles). For the PBMA-labeled polymer, $T_{g,E}$ = 295 K and $T_{g,J}$ = 303 K, representing only an 8 K range in local T_g along the PBMA block. As a benchmark, recall that the PMMA and PBMA homopolymers have a 96 K difference in bulk T_g.

A powerful feature of fluorescence as an approach to measure T_g is that the reporter dye labels can be placed at prescribed locations along the chain, as schematically illustrated in Figure 2a. This provides a unique means to probe the full gradient of glass-to-rubber transition temperatures within the self-assembled diblock copolymer. However, the distribution of distances of the fluorescent label from the block interface must be evaluated. Here, self-consistent field theory (SCFT) calculations, correcting for fluctuations via renormalized one-loop theory, were used to accomplish this task (see the SI for details). The spatial distribution of monomer segments at selected positions along the chain was calculated using open source code created by Arora and co-workers.[24] Figure 3 shows

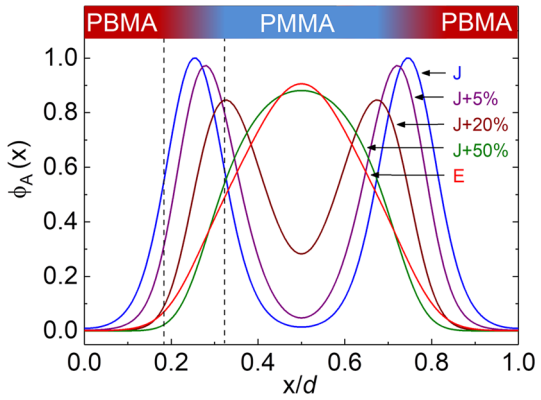

Figure 3. Composition profile of labeled segments across the domain period (d) of a symmetric diblock copolymer where $\chi N/(\chi N)_{ODT}$ = 2.4, for the five different label positions schematized in Figure 2a. Profiles have been smeared with a displacement σ = 0.029 (see the SI for details). Dashed vertical lines demarcate the width of the interface as determined by SAXS. Profiles are normalized to equal area, with the highest value of labeled segment density (ϕ_A) set to unity.

the calculated composition profiles for the pyrene-bearing segments across the domain period of a symmetric diblock copolymer with $\chi N/(\chi N)_{ODT}$ = 2.4, where d is the domain period and x is the distance along the lamellar normal, starting from the center of the PBMA-rich domain (x/d = 0, 1). A value of d = 27 nm was determined for a PBMA–PMMA diblock copolymer with M = 47 kg/mol by small-angle X-ray scattering (SAXS) (see Figure S6d). Vertical dashed lines in Figure 3 represent the thickness of the interface (t = 3.8 nm) determined by SAXS.

The calculated composition profiles highlight that the location of the pyrene labels within the self-assembled nanodomain structure can be controlled and tuned. For instance, placement of the pyrene labels at the PMMA chain end resulted in a composition profile (red curve) whose maximum is in the center of the PMMA-rich domain. Conversely, placement of the pyrene labels at the block junction revealed a composition profile (blue curve) whose maximum is at the block junction, i.e., the center of the polymer–polymer interface. Collectively, the T_g determined for selectively labeled segments, the evaluation of the segment distribution, and the measurement of the domain period allowed us to map T_g across the domain structure of the self-assembled diblock copolymer with nanometer accuracy.

Figure 4 plots the local T_g within the diblock copolymer, as a function of average distance from the nearest PBMA–PMMA

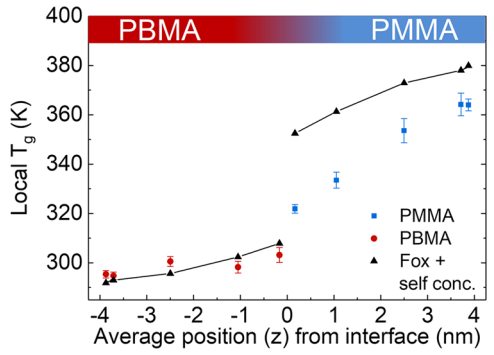

Figure 4. Experimental T_g as a function of average position across the domain period of a lamellar PBMA–PMMA diblock copolymer, where $\chi N/(\chi N)_{ODT}$ = 2.4: PBMA (red) or PMMA (blue) segments. The black symbols correspond to the calculated T_g of PBMA (left) or PMMA (right) segments, using the Fox equation and accounting for self-concentration effects ($\phi_{s,PMMA}$ = 0.38 and $\phi_{s,PBMA}$ = 0.5).

interface, z (z/d = 0, 0.25), over one-half of the domain period. The PBMA–PMMA block junction is identified as z = 0 nm. The local T_g was measured for five label locations along each block, as highlighted in Figure 2a. As illustrated in Figure 3, the pyrene labels have some distribution in space (typically a few nm), and the measured T_g reflects an average over this distribution. For Figure 4, the position (z) of the label from the interface, corresponding to the measured T_g for each label location along the chain, was taken to be the concentration-average position[25] of the respective labeled segment composition profile (Figure 3, see Figure S10 for additional discussion). Remarkably, the 42 K variation in T_g noted above occurs across only a 4 nm distance. While classical measurements, such as DSC or broadband dielectric spectroscopy, have revealed heterogeneous dynamics within the nanodomain structure,[26−28] the present fluorescence measurements are the first to quantify the spatial variation and gradients governing said dynamics in block copolymers.

In the case of the rubbery-glassy PBMA–PMMA diblock copolymer, a highly asymmetric gradient in T_g about the interface was observed. Within the PBMA domain, $T_{g,E}$ = 295 K at the chain end, i.e., z = −4 nm. This value was also consistent with the T_g measured by fluorescence for the uniformly labeled PBMA block, $T_{g,U}$ = 296 K. Across the PBMA domain, an 8 K range in PBMA T_g was observed. In contrast, within the PMMA

DOI: 10.1021/acscentsci.8b00043
ACS Cent. Sci. 2018, 4, 504−511

domain, $T_{g,E}$ = 364 K at the chain end, i.e., z = +4 nm, which is also consistent with the T_g measured for the uniformly labeled PMMA block, $T_{g,U}$ = 362 K. However, across the PMMA domain, a 42 K range in PMMA T_g was observed. Thus, the magnitude of the perturbation of the dynamics by the interface was much greater in the glassy domain than in the rubbery domain. This is qualitatively consistent with the fluorescence results of Baglay and Roth[29] on multilayer films, wherein a greater T_g perturbation was observed for a thin film sandwiched between rubbery layers than between glassy layers.

There are several key observations from the measurements presented in Figures 2 and 4: (i) within each self-assembled nanodomain there exists a strongly location-dependent T_g, (ii) the ΔT_g ($T_{g,E} - T_{g,J}$) has a larger magnitude in the PMMA domain in comparison to the PBMA domain, and (iii) there is a 19 K difference in $T_{g,J}$ depending on whether the pyrene label is located within the PMMA or PBMA block, adjacent to the block junction. These observations combine to highlight a complex interplay between interfacial and self-concentration effects on the dynamics of nanostructured polymers, as discussed below.

To better understand these observations, a location-dependent T_g was calculated based on the LM model, with $\phi_{s,PMMA}$ = 0.38 and $\phi_{s,PBMA}$ = 0.5, using the local composition (ϕ) calculated by SCFT at each position along the domain period. If the dynamics were dependent only on the local composition, and if there were no additional influences of the domain interfaces, then the LM model would be expected to accurately capture the spatial variation of T_g across the domain period. The ϕ_{eff} and T_g profiles were then computed via eqs 1 and 2 (see Figure S8). The effective T_g experienced by a labeled segment was determined by linearly weighting the effective T_g by the labeled segment distribution[25] (Figure 3) and is also plotted in Figure 4 (black triangles); black connecting lines represent a guide to the eye. The validity of linearly weighting the effective T_g by the labeled segment distribution was confirmed by summing the labeled segment distributions with weights that yielded a close match to the composition profile within the PMMA block for the uniformly labeled PMMA block, and using those weighting factors to calculate $T_{g,U}$ based on the measured T_g values corresponding to each segment distribution (Figure 4, see Figure S9 and Table S3). The $T_{g,U}$ determined from this calculation was 359 K, in good agreement with the experimental $T_{g,U}$ = 362 K of the diblock copolymer with a uniformly labeled PMMA block.

Self-concentration can qualitatively account for the dissimilar T_g values measured for the two junction-labeled polymers, depending on whether the label was incorporated on the PBMA or PMMA side of the junction, since each component is locally enriched in its own type of segment. Moreover, the more compact coils formed by PBMA (higher ϕ_s) led to a smaller range of T_g experienced by the PBMA block than the PMMA block. Self-concentration also accounts for the spatial variation of the local T_g in the PBMA block, as noted by the good agreement between the experimental and calculated values. In contrast, for the PMMA block, the experimentally determined T_g was systematically lower than the value predicted by the LM model, even in the domain center. While the LM model considers self-concentration effects on T_g, it does not account for changes in T_g that could occur due to nanoscale confinement. We therefore attribute the local T_g profile within the PMMA domain to segmental mixing modulated by self-concentration, crucially combined with the presence of interfaces, which lead to nanoscale confinement and a reduction in T_g within the thin block copolymer domains.

It is well-known that in states of soft confinement, where interfacial effects become important, PMMA exhibits a suppression in T_g relative to the bulk.[30,31] In considering the effects observed here, the significantly lower T_g within the PMMA domain can be explained via soft confinement by the PBMA block which imparts additional mobility, originating at the domain interface, to the PMMA blocks. As such, the bulk value of T_g for PMMA is not recovered even in the center of the PMMA domain due to interface-induced gradients in T_g, which may propagate over distances of tens[14,32] or even hundreds[29,33] of nanometers, i.e., much greater than the domain size. The agreement between T_g as determined by fluorescence and the LM model in the PBMA-rich domain can similarly be explained within the context of nanoscale confinement. The glassy PMMA domain, which confines PBMA, acts as a solid substrate with no attractive interactions and represents the case of hard confinement. Under this circumstance, bulk values of T_g are expected and observed, in agreement with prior examples of polymers subject to hard confinement.[34−36]

The influence of interblock segregation strength on the local dynamics was assessed by a comparison of the local T_g of the PMMA block at weak (M = 26 ± 2 kg/mol, $Đ \leq$ 1.06, $\chi N/(\chi N)_{ODT}$ = 1.2) and intermediate (M = 54 ± 9 kg/mol, $Đ \leq$ 1.1, $\chi N/(\chi N)_{ODT}$ = 2.4) segregation strengths. Figure 5 shows

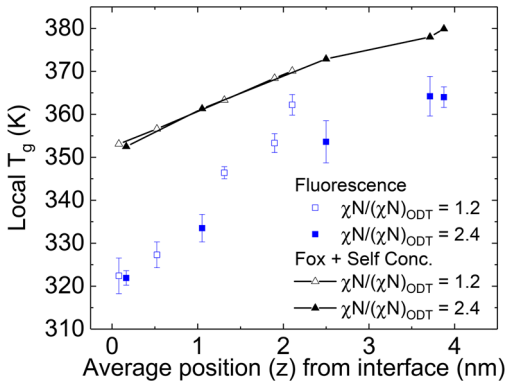

Figure 5. T_g as a function of distance from the interface as measured by fluorimetry (squares) or calculated via the LM model (triangles) at weak (open symbols) and intermediate (closed symbols) segregation strengths.

the local T_g for the PMMA block, as determined by fluorimetry and as calculated by the LM model, at weak and intermediate segregation strengths vs the average position of a labeled monomer segment. The pyrene-bearing monomer was placed at the same fractional distance, e.g., J + 50%, for both sets of diblock copolymers. Although the segment density profiles are significantly broader at weak segregation (Figure S11) vs intermediate segregation (Figure 3), the local T_g as calculated by the LM model, averaged over the segment density distribution, is quite similar for the two segregation strengths at any value of z. At the block interface, in both weak and intermediate segregation, the PMMA blocks exhibit roughly a 30 K depression in T_g relative to the calculated value. In the center of the domain the difference in T_g between the experimental and calculated values, though smaller than that at

DOI: 10.1021/acscentsci.8b00043
ACS Cent. Sci. 2018, 4, 504−511

the interface (~10 K vs ~30 K), persists for both segregation strengths.

CONCLUSIONS

This study has demonstrated the utility of fluorescence spectroscopy to characterize the glass transition in multicomponent polymers over different length scales where segmental mixing, self-concentration, and interfacial effects act to perturb T_g. In homogeneous diblock copolymers, we characterized the dynamics of one type of block and demonstrated the presence of self-concentration effects, which are active over the distance of a few monomer units. In nanostructured diblock copolymers, both interfacial and self-concentration effects act to perturb T_g yielding an asymmetric T_g variation across the interface. The location-specific nature of fluorescence spectroscopy to characterize T_g was highlighted, as gradients in nanostructured polymers over length scales less than 5 nm were characterized with nanometer spatial resolution. Insights gained from the nanometer-scale measurements of T_g will inform the design of nanostructured polymers for emerging applications where control of interfacial dynamics has been shown to enhance performance, e.g., block copolymer electrolytes for solid-state batteries.[37,38]

METHODS

Fluorescent Label and Polymer Synthesis. The fluorescent label, 1-pyrenylbutyl methacrylate, was synthesized via the condensation of methacryloyl chloride (Sigma-Aldrich) and 1-pyrenebutanol (Sigma-Aldrich).[14] A mixture (4:4:1 stoichiometric ratio) of triethyl amine, methacryloyl chloride, and 1-pyrenebutanol, respectively, in tetrahydrofuran (THF) was stirred under nitrogen at 195 K for 12 h. The crude product was dissolved in toluene, washed with an aqueous solution of sodium hydrogen carbonate (Fisher Scientific) to remove amine salts, and finally purified by recrystallization.

The synthesis of labeled homopolymers and diblock copolymers was achieved via anionic polymerization.[39] Monomers and solvent (THF) were rigorously treated to remove impurities, water, and oxygen. Butyl and methyl methacrylate monomers (Sigma-Aldrich) were purified by first removing most of the oxygen via freeze−pump−thaw (FPT) cycles. The monomer was then stirred over trioctylaluminum (Sigma-Aldrich), added under nitrogen flow, to react with any protic impurities.[40] Next, nitrogen was removed via FPT cycles and the monomer was short-path vacuum transferred to a storage vessel and kept in a glovebox (MBRAUN UNIlab, < 0.1 ppm of H_2O and O_2) freezer. All polymerizations were carried out in THF, delivered from an MBRAUN compact solvent purification system, in the coldwell of the glovebox, which was cooled by an external dry ice−isopropanol bath at 195 K.

The polymerization conditions described below apply to the synthesis of both labeled homopolymers and diblock copolymers. A glass reactor rinsed with *sec*-butyllithium (*s*-BuLi, Sigma-Aldrich) was filled with clean THF (20:1 solvent to monomer volume ratio) and cooled to 195 K. Lithium chloride (LiCl, Sigma-Aldrich) and diphenylethylene (DPE, Sigma-Aldrich) were added to the reactor in a 10:1 LiCl:*s*-BuLi mole ratio and 3:1 DPE:*s*-BuLi mole ratio. LiCl was added to minimize attack on the C═O bond.[38] DPE was added to form a sterically hindered initiator with *s*-BuLi. Prior to starting polymerization, the reactor containing THF, LiCl, and DPE was titrated with *s*-BuLi until a red color persisted. Next, a predetermined amount, based on the target molecular weight and polymer batch size, of *s*-BuLi was added to the reactor. For the synthesis of labeled homopolymers, a mixture of labeled and unlabeled monomer was added to the reactor in a dropwise manner over a period of 1−2 min, allowed to react for 10 min, and then terminated by the addition of methanol, which capped the chain with a proton. A reaction time of 10 min was well in excess of the time required for essentially complete conversion (>99%) of the monomer.[41]

The synthesis of diblock copolymers of PBMA−PMMA is analogous to that described above for PMMA homopolymer; the PBMA block was polymerized first. The type and number of necessary monomer charges depend on the desired location of the label in the product, but in all cases, 10 min was allowed for the propagation after each monomer charge. For diblock copolymers labeled at specific positions along the chain, only 1% of the respective block was labeled. The label was added at trace levels, i.e., < 0.5 mol % of any monomer charge. This translates to a typical value of three labeled monomers per chain for the uniform labeling case; for the copolymers labeled at specific positions along the chain, this translates to approximately one label per 30 chains. All polymers were recovered postsynthesis by precipitation into methanol and then drying in a vacuum oven.

Molecular Characterization. The polymer molecular weights and dispersities ($Đ$) were characterized by gel permeation chromatography (GPC). The GPC system employed a model 515 pump (Waters) delivering THF mobile phase at 1 mL/min, two PLgel Mixed-C 30 cm columns (Agilent) operated at 308 K, a miniDAWN TREOS light scattering (LS) detector (Wyatt Technologies, 658 nm, room temperature), an Optilab T-rEX differential refractive index (DRI) detector (Wyatt Technologies, 658 nm, 298 K), and a Model 2487 Dual-Wavelength UV−visible absorbance detector (Waters). Polymer dispersity was measured using the DRI signal, with the elution times calibrated with narrow-distribution polystyrene standards. The true weight-average molecular weight of homopolymers of PMMA and PBMA was characterized by LS with specific refractive index increments (dn/dc) measured independently on an Optilab rEX differential refractometer (Wyatt Technologies): 0.0818 and 0.0763 mL/g for PMMA and PBMA in THF at 298 K and λ = 658 nm, respectively. For diblock copolymers, the true weight-average molecular weight was characterized by LS using a weight-fraction-weighted dn/dc.[42] In all cases the weight-average molecular weight from LS was divided by $Đ$ from the DRI signal to yield the number-average molecular weight M, reported herein. The composition of each diblock copolymer was determined by proton nuclear magnetic resonance (^{1}H NMR) in chloroform-*d* using a Bruker AVANCE III spectrometer operating at 500 MHz. The relative intensity of the resonances corresponding to the O−CH_3 and O−CH_2− protons of PMMA and PBMA, located at δ = 3.6 ppm and δ = 3.93 ppm, respectively, defined the diblock copolymer composition. The purity of 1-pyrenylbutyl methacrylate monomer was also characterized by ^{1}H NMR.

Morphological Characterization. Small-angle X-ray scattering (SAXS) patterns were collected in transmission using nickel-filtered Cu Kα radiation from a PANalytical PW3830 generator with a PANalytical C-Tech long fine focus tube, a compact Kratky camera (Anton-Paar), and a BRAUN OED-50 M one-dimensional position-sensitive detector.

DOI: 10.1021/acscentsci.8b00043
ACS Cent. Sci. 2018, 4, 504−511

Samples were mounted into a home-built hot stage, held in copper cells between mica windows. Data were corrected for empty beam scattering, detector sensitivity, positional linearity, sample thickness, and transmittance and were desmeared for slit length.[43] Absolute scattering intensities (I/I_eV) were obtained based on a polyethylene standard and plotted as a function of the magnitude of the momentum transfer vector, $q = (4\pi/\lambda)\sin\theta$, where θ is half the scattering angle.

T_g Measurement. The bulk T_g values of homopolymers of PBMA and PMMA and diblock copolymers of PBMA−PMMA were measured using differential scanning calorimetry (TA Instruments Q2000, second heating at a heating rate of 2 K/min) calibrated with sapphire and indium standards. A typical run employed a 7 mg polymer sample. All reported $T_{g,Bulk}$ values correspond to the transition onset defined as the intersection of the glassy line and transition line of a calorimetric thermogram (see Figure S5). The fluorimetric T_g was characterized on spin-coated or dropcast films deposited onto a silica substrate (VG-9 glass, Schott, North America) at ∼10 μm thicknesses. The films were annealed at $T_{g,Bulk}$ + 30 K for 12 h. The fluorescence emission intensity was measured using a Fluorolog-3 spectrofluorimeter (Horiba Scientific). A typical measurement consists of rapidly heating a film to $T_{g,Bulk}$ + 20 K (±10 K), maintaining an isotherm for 20 min to remove the processing history of the film, then collecting the steady-state fluorescence emission spectrum at 5 K intervals at a 1 or 2 K/min cooling rate. The pyrene labels were excited at 347 nm with a 1 nm bandpass. The emission spectra were collected over the range of 350−500 nm.

■ ASSOCIATED CONTENT

Supporting Information

The Supporting Information is available free of charge on the ACS Publications website at DOI: 10.1021/acscentsci.8b00043.

Molecular characterization, thermal characterization (DSC and fluorimetry), estimation of χN, fluctuation correction to the SCFT composition profiles, estimation of self-concentration fractions (ϕ_s), effective composition profiles and local T_g, validity of linearly weighting monomer segment distributions, monomer segment distributions, and average monomer segment positions (PDF)

■ AUTHOR INFORMATION

Corresponding Authors

*E-mail: register@princeton.edu.
*E-mail: rpriestl@princeton.edu.

ORCID

Richard A. Register: 0000-0002-5223-4306
Rodney D. Priestley: 0000-0001-6765-2933

Notes

The authors declare no competing financial interest.

■ ACKNOWLEDGMENTS

This work was supported by the National Science Foundation (NSF) Materials Research Science and Engineering Center Program through the Princeton Center for Complex Materials (DMR-1420541). D.C. acknowledges the support of an NSF graduate research fellowship. R.D.P. acknowledges the AFOSR through a PECASE Award (FA9550-12-1-0223).

■ REFERENCES

(1) Bates, C. M.; Bates, F. S. 50th anniversary perspective: Block polymers—pure potential. *Macromolecules* **2017**, *50*, 3−22.
(2) Ediger, M. D.; Forrest, J. A. Dynamics near free surfaces and the glass transition in thin polymer films: a view to the future. *Macromolecules* **2014**, *47*, 471−478.
(3) McKenna, G. B. Ten (or more) years of dynamics in confinement: Perspectives for 2010. *Eur. Phys. J.: Spec. Top.* **2010**, *189*, 285−302.
(4) Forrest, J. A.; Dalnoki-Veress, K. The glass transition in thin polymer films. *Adv. Colloid Interface Sci.* **2001**, *94*, 167−196.
(5) Simmons, D. S. An emerging unified view of dynamic interphases in polymers. *Macromol. Chem. Phys.* **2016**, *217*, 137−148.
(6) Jouenne, S.; González-Léon, J. A.; Ruzette, A.-V.; Lodéfier, P.; Leibler, L. Styrene−butadiene gradient block copolymers for transparent impact polystyrene. *Macromolecules* **2008**, *41*, 9823−9830.
(7) Eagan, J. M.; Xu, J.; Di Girolamo, R.; Thurber, C. M.; Macosko, C. W.; LaPointe, A. M.; Bates, F. S.; Coates, G. W. Combining polyethylene and polypropylene: Enhanced performance with PE/iPP multiblock polymers. *Science* **2017**, *355*, 814−816.
(8) Chen, Y.; Kushner, A. M.; Williams, G. A.; Guan, Z. Multiphase design of autonomic self-healing thermoplastic elastomers. *Nat. Chem.* **2012**, *4*, 467−472.
(9) Tao, Y.; McCulloch, B.; Kim, S.; Segalman, R. A. The relationship between morphology and performance of donor−acceptor rod−coil block copolymer solar cells. *Soft Matter* **2009**, *5*, 4219−4230.
(10) Sivula, K.; Ball, Z. T.; Watanabe, N.; Fréchet, J. M. J. Amphiphilic diblock copolymer compatibilizers and their effect on the morphology and performance of polythiophene: fullerene solar cells. *Adv. Mater.* **2006**, *18*, 206−210.
(11) Glaser, J.; Medapuram, P.; Beardsley, T. M.; Matsen, M. W.; Morse, D. C. Universality of block copolymer melts. *Phys. Rev. Lett.* **2014**, *113*, 068302.
(12) Matsen, M. W.; Bates, F. S. Unifying weak-and strong-segregation block copolymer theories. *Macromolecules* **1996**, *29*, 1091−1098.
(13) Fox, T. G., Jr.; Flory, P. J. Second-order transition temperatures and related properties of polystyrene. I. Influence of molecular weight. *J. Appl. Phys.* **1950**, *21*, 581−591.
(14) Ellison, C. J.; Torkelson, J. M. The distribution of glass-transition temperatures in nanoscopically confined glass formers. *Nat. Mater.* **2003**, *2*, 695−700.
(15) Ellison, C. J.; Torkelson, J. M. Sensing the glass transition in thin and ultrathin polymer films via fluorescence probes and labels. *J. Polym. Sci., Part B: Polym. Phys.* **2002**, *40*, 2745−2758.
(16) Burroughs, M. J.; Napolitano, S.; Cangialosi, D.; Priestley, R. D. Direct measurement of glass transition temperature in exposed and buried adsorbed polymer nanolayers. *Macromolecules* **2016**, *49*, 4647−4655.
(17) Priestley, R. D.; Mundra, M. K.; Barnett, N. J.; Broadbelt, L. J.; Torkelson, J. M. Effects of nanoscale confinement and interfaces on the glass transition temperatures of a series of poly (n-methacrylate) films. *Aust. J. Chem.* **2007**, *60*, 765−771.
(18) Thompson, E. V. Dependence of the glass transition temperature of poly (methyl methacrylate) on tacticity and molecular weight. *J. Polym. Sci. A-2* **1966**, *4*, 199−208.
(19) Mok, M. M.; Lodge, T. P. Temperature-based fluorescence measurements of pyrene in block copolymer micelles: Probing micelle core glass transition breadths. *J. Polym. Sci., Part B: Polym. Phys.* **2012**, *50*, 500−515.
(20) Wei, W.-C.; Feng, S.; Zheng, C.-X.; Liang, G.-D.; Gao, H.-Y.; Wu, Q.; Zhu, F.-M. Glass transition and quantum yield for fluorescent labelled polystyrene core-forming block in self-assembled nanomicelles of amphiphilic diblock copolymers. *J. Polym. Res.* **2015**, *22*, 212.
(21) Mundra, M. K.; Ellison, C. J.; Rittigstein, P.; Torkelson, J. M. Fluorescence studies of confinement in polymer films and nanocomposites: glass transition temperature, plasticizer effects, and sensitivity to stress relaxation and local polarity. *Eur. Phys. J.: Spec. Top.* **2007**, *141*, 143−151.

DOI: 10.1021/acscentsci.8b00043
ACS Cent. Sci. 2018, 4, 504−511

(22) Fox, T. G. Influence of diluent and of copolymer composition on the glass temperature of a polymer system. *Bull. Am. Phys. Soc.* **1956**, *1*, 123.
(23) Lodge, T. P.; McLeish, T. C. B. Self-concentrations and effective glass transition temperatures in polymer blends. *Macromolecules* **2000**, *33*, 5278−5284.
(24) Arora, A.; Qin, J.; Morse, D. C.; Delaney, K. T.; Fredrickson, G. H.; Bates, F. S.; Dorfman, K. D. Broadly accessible self-consistent field theory for block polymer materials discovery. *Macromolecules* **2016**, *49*, 4675−4690.
(25) Sethuraman, V.; Ganesan, V. On the relationship between the local segmental dynamics and the tagged monomer dynamics in lamellar phases of diblock copolymers. *J. Chem. Phys.* **2017**, *147*, 104901.
(26) Kříž, J.; Pleštil, J.; Tuzar, Z.; Pospíšil, H.; Brus, J.; Jakeš, J.; Masař, B.; Vlček, P.; Doskočilová, D. Interface affected polymer dynamics: NMR, SANS, and DLS study of the influence of shell−core interactions on the core chain mobility of poly(2-ethylhexyl acrylate)-*block*-poly(acrylic acid) micelles in water. *Macromolecules* **1999**, *32*, 397−410.
(27) Lund, R.; Willner, L.; Alegría, A.; Colmenero, J.; Richter, D. Self-concentration and interfacial fluctuation effects on the local segmental dynamics of nanostructured diblock copolymer melts. *Macromolecules* **2008**, *41*, 511−514.
(28) Gaur, U.; Wunderlich, B. Study of microphase separation in block copolymers of styrene and α-methylstyrene in the glass transition region using quantitative thermal analysis. *Macromolecules* **1980**, *13*, 1618−1625.
(29) Baglay, R. R.; Roth, C. B. Local glass transition temperature T-g(z) of polystyrene next to different polymers: Hard vs. soft confinement. *J. Chem. Phys.* **2017**, *146*, 203307.
(30) Keddie, J. L.; Jones, R. A. L.; Cory, R. A. Interface and surface effects on the glass-transition temperature in thin polymer films. *Faraday Discuss.* **1994**, *98*, 219−230.
(31) Roth, C. B.; Dutcher, J. R. Glass transition temperature of freely-standing films of atactic poly (methyl methacrylate). *Eur. Phys. J. E: Soft Matter Biol. Phys.* **2003**, *12*, 103−107.
(32) Evans, C. M.; Kim, S.; Roth, C. B.; Priestley, R. D.; Broadbelt, L. J.; Torkelson, J. M. Role of neighboring domains in determining the magnitude and direction of T_g-confinement effects in binary, immiscible polymer systems. *Polymer* **2015**, *80*, 180−187.
(33) Baglay, R. R.; Roth, C. B. Experimentally determined profile of local glass transition temperature across a glassy-rubbery polymer interface with a T_g difference of 80 K. *J. Chem. Phys.* **2015**, *143*, 111101.
(34) Zhang, C.; Guo, Y. L.; Priestley, R. D. Glass transition temperature of polymer nanoparticles under soft and hard confinement. *Macromolecules* **2011**, *44*, 4001−4006.
(35) Forrest, J. A.; Dalnoki-Veress, K.; Dutcher, J. R. Interface and chain confinement effects on the glass transition temperature of thin polymer films. *Phys. Rev. E: Stat. Phys., Plasmas, Fluids, Relat. Interdiscip. Top.* **1997**, *56*, 5705−5716.
(36) Sanz, A.; Nogales, A.; Ezquerra, T. A. From hard to soft confinement in a symmetric block copolymer: local and segmental dynamics. *Soft Matter* **2011**, *7*, 6477−6483.
(37) Kuan, W.-F.; Remy, R.; Mackay, M. E.; Epps, T. H., III Controlled ionic conductivity via tapered block polymer electrolytes. *RSC Adv.* **2015**, *5*, 12597−12604.
(38) Morris, M. A.; Gartner, T. E.; Epps, T. H., III Tuning block polymer structure, properties, and processability for the design of efficient nanostructured materials systems. *Macromol. Chem. Phys.* **2017**, *218*, 1600513.
(39) Kwon, H. K.; Lopez, V. E.; Davis, R. L.; Kim, S. Y.; Burns, A. B.; Register, R. A. Polystyrene-poly(2-ethylhexylmethacrylate) block copolymers: Synthesis, bulk phase behavior, and thin film structure. *Polymer* **2014**, *55*, 2059−2067.
(40) Allen, R. D.; Long, T. E.; McGrath, J. E. Preparation of high purity, anionic polymerization grade alkyl methacrylate monomers. *Polym. Bull.* **1986**, *15*, 127−134.
(41) Varshney, S. K.; Hautekeer, J. P.; Fayt, R.; Jérôme, R.; Teyssié, P. Anionic polymerization of (meth)acrylic monomers. 4. Effect of lithium salts as ligands on the ″living″ polymerization of methyl methacrylate using monofunctional initiators. *Macromolecules* **1990**, *23*, 2618−2622.
(42) Bushuk, W.; Benoît, H. Light-scattering studies of copolymers: I. Effect of heterogeneity of chain composition on the molecular weight. *Can. J. Chem.* **1958**, *36*, 1616−1626.
(43) Register, R. A.; Bell, T. R. Miscible blends of zinc-neutralized sulfonated polystyrene and poly(2,6-dimethyl 1,4-phenylene oxide). *J. Polym. Sci., Part B: Polym. Phys.* **1992**, *30*, 569−575.

DOI: 10.1021/acscentsci.8b00043
ACS Cent. Sci. 2018, 4, 504−511